Topography-based Modelling of Soil Moisture Using LiDAR-derived High-resolution Digital Elevation Models

Noah GREUPNER[1]

[1]Z_GIS, University of Salzburg, Austria · noah.greupner@stud.plus.ac.at

Abstract

Soil moisture (SM) is a crucial hydrological variable essential for ecosystem functioning and the provision of ecosystem services. Given its strong relationship with terrain characteristics, Digital Elevation Model (DEM)-based indices are increasingly used to estimate SM across different ecosystems. However, a comprehensive comparison of these indices, particularly at a local scale and using high-resolution DEMs, is lacking. This study aims to compare three topography-based indices for spatiotemporal soil moisture modelling in the Salzach river floodplains in Austria. I utilized LiDAR-derived high-resolution DEMs (1m) from 2016 and 2022 to calculate the Depth-to-Water, Height-Above-the-Nearest-Drainage, and SAGA Wetness Index maps. These maps were aggregated and statistically compared. The findings reveal a heterogeneous SM pattern in the study area, with strong correlations between the Depth-to-Water and Height-Above-the-Nearest-Drainage indices, while moderate correlations were observed between the SAGA Wetness Index and the other two indices. Temporal changes between the two years were not statistically significant. Further evaluation with field data, an analysis of the influence of the Flow Initiation Area (FIA) on the resulting SM maps and the incorporation of additional site parameters and seasonal dynamics could enhance the accuracy and applicability of these indices. The results of this research are valuable for environmental planning and management, contributing to improved decision-making and conservation of floodplain ecosystems in Austria.

1 Introduction

Soil moisture serves as a pivotal ecosystem condition variable that shapes ecosystem functioning in floodplains and riparian forests (Yin et al., 2019). Thus, precise and spatially explicit SM monitoring is indispensable for effective environmental management on different spatial scales. To estimate SM conditions, DEM-based techniques have seen a rise in development and application (Larson et al., 2022), with several advantages over optical remote sensing, such as less data intensity and the applicability to forested areas (Larson et al., 2022). As topography is one of the key factors influencing hydrological pathways and hence SM (Bell et al., 1992; Famiglietti et al., 1998), topography-based indices assume lower areas near water sources typically to be wetter than higher areas further away from these sources (Nobre et al., 2011).

The Topographic Wetness Index (TWI) was one of the first indices in this field (Beven & Kirkby, 1979). It has been employed in SM modelling over various ecosystems (Moore et al., 1993), indicating the likelihood of an area accumulating water. Regions with extensive contributing drainage areas and gentle slopes are linked to high TWI values, suggesting a greater potential for SM accumulation. In contrast, steep, well-drained areas exhibit low TWI values. The SAGA Wetness Index (SWI), developed by Böhner and Selige (2002), modifies the TWI by adjusting the computation of the specific catchment area. Rather than treating the flow as a thin film, it provides a more realistic representation of SM potential by considering cells in valley bottoms with minimal vertical distance to a channel.

In recent times, the Depth-to-Water (DTW) index, as first described by Murphy et al. (2007), has been used for riparian and peatland soil wetness mapping in research and public authorities in Scandinavia and Canada (Lidberg et al., 2020; Mohtashami et al., 2022). DTW describes the elevation difference (m) to the nearest surface water source along the cumulative least-cost slope path and, thereby, identifies low-lying areas susceptible to surface saturation (Schönauer et al., 2024). Similar to the DTW, the Height-Above-the-Nearest-Drainage (HAND) index, developed by Rennó et al. (2008), is also described as the vertical elevation difference between a point in the landscape and the nearest surface water source. However, HAND is computed using the downslope flow path. Originally developed for Amazon regions, it is now incorporated into several models for improved flood forecast such as the integrated National Water Model –Height Above Nearest Drainage (NWM–HAND) flood mapping approach (Johnson et al., 2019).

While the three indices have already proven their suitability in wetlands of different climates, a comprehensive spatiotemporal comparison between them is still missing, especially in temperate regions. In addition to that, studies have already proven the applicability of DTW and HAND with high-resolution DEMs at regional and national levels (Ågren et al., 2021; Mohtashami et al., 2022), but there is less evidence for their utility on local scales. This study, therefore, aims to compare DTW, HAND and SAGA Wetness Index maps on a small scale in the Salzach river floodplains. Consequently, the following research questions are addressed: **a)** To what extent are observed indices suitable for small-scale high-resolution SM modelling in floodplain ecosystems and what differences can be observed between them? **b)** What is the spatiotemporal variability of SM as depicted by the three indices in the study area? To answer the research questions, high-resolution DEMs of the study area are obtained for the years 2016 and 2022. The resulting index rasters are further aggregated and statistically evaluated.

2 Material and Methods

2.1 Salzach river floodplains

The test site for this study covers the Weithwörth floodplain and the Anthering floodplain which are located in the Salzach river floodplains (Salzburg, Austria; UL: N 47°56’12” / E 12°56’24”; LR: N 47°52’17” / E 13°00’22”) (Fig. 1). The area is a semi-natural Natura 2000

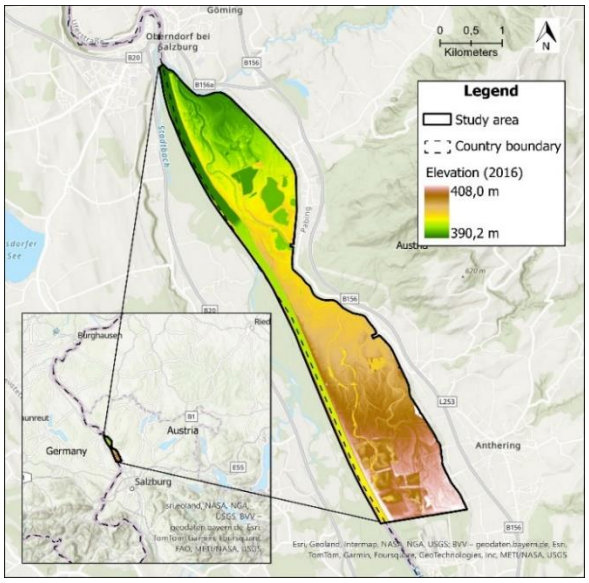

Figure 1: Study area.

site, which has recently undergone renaturation measures as part of an EU-funded LIFE project, enabling more natural hydrodynamic conditions (Hengl et al., 2012). The site mainly consists of riparian forests and represents a habitat for endangered birds and amphibians (Strasser & Lang, 2015). The soil in the area is characterized by gleyed, calcareous brown alluvial soil composed of fine alluvial deposits of the Salzach (BFW, 2023). The SM varies from moderately moist to wet, with moderate water storage capacity and permeability. Certain areas experience persistent wetness due to a constantly high groundwater level. The soil texture ranges from silt to sandy silt, with occasional occurrences of loamy silt.

2.2 Data sources

High-resolution Digital Elevation Models and vector stream data were used as the basis for deriving the SM maps. The DEMs were obtained from the Federal State of Salzburg (SAGIS). They are derived from airborne laser scanning data and obtained for the years 2016 and 2022. The DEMs have a spatial resolution of 0.5 and 1 meter and are provided in GeoTIFF format. Before conducting the actual pre-processing steps, the DEM data was merged, resampled to 1 meter (bilinear resampling) and clipped to the boundary of the study area which had been buffered by 100 meters. This avoids potential edge effects when calculating the indices. After index calculation, the buffered area was clipped to the actual study area size.

The vector stream data was obtained from the Austrian Federal Office for Metrology and Surveying (BEV), clipped to the study area and used for stream burning.

2.3 Data pre-processing and stream extraction

To use the DEMs for hydrological modelling, they must first be corrected using pre-processing steps which were conducted in ArcGIS (Version 3.3.0).

First, the *fillburn* algorithm from the Whitebox Geospatial Analysis Tools (GAT) was utilised. This function was used to burn the vector stream data into the DEM, which has been shown to improve the overall accuracy of the results (Lidberg et al., 2017). Simultaneously, sinks were filled, which represents a widely known method accounting for natural depressions or artefacts which potentially distort the generation of downstream flow paths

(Lindsay, 2016). Filling was preferred over breaching algorithms because the study area lacks anthropogenic features for which breaching would be more appropriate (Lidberg et al., 2017).

Subsequently, flow direction and flow accumulation were derived from the hydrologically corrected DEMs. The Deterministic-8 (D8) method was employed for this purpose (O'Callaghan & Mark, 1984), as there are only minor accuracy differences compared to more complex methods when applied to DEMs of high resolution (Lidberg et al., 2017). A flow initiation area (FIA) of 0.5 hectares was set to extract streams from the flow accumulation raster, aligning with threshold ranges used in studies with similar spatial resolution (Ågren et al., 2021). This relatively low FIA is appropriate for analyses of small-scale areas which incorporate high-resolution DEMs (Bhowmik et al., 2015). Furthermore, a low FIA helps to consider the small watercourses and hydrological connectivity typical wetlands that official stream data often miss (Ågren & Lidberg, 2019).

2.4 Index calculation

After pre-processing and stream extraction steps, the indices were calculated using ArcGIS Pro (Version 3.3.0) and SAGA GIS (Version 7.8.2). The SAGA Wetness Index was calculated using the eponymous module in SAGA GIS. It describes the tendency of a cell to be wet, based on Eq. 1, where SCA_M represents the specific catchment area and *ß* represents the slope of the grid cells in degrees (Böhner & Selige, 2002).

$$(1) \quad WI_s = \ln\left(\frac{SCA_M}{\tan\beta}\right)$$

A modified approach by Schönauer et al. (2021) was followed to calculate DTW, as automated tools for DTW calculation are not publicly available. The DTW index is defined as the cumulative slope along the least-cost path from a cell in the landscape to the nearest flow channel (Murphy et al., 2007), described by Eq. 2.

$$(2) \quad DTW\ (m) = \left[\sum \frac{dz_i}{dx_i}\right] xc$$

A slope map was derived from the original (not hydrologically corrected) DEM and used with the stream raster as input for the *Accumulated Cost* module in SAGA GIS to produce the DTW raster.

HAND was calculated using the *Topography Toolbox Pro* from Dilts (2023) in ArcGIS Pro. It is defined as the elevation difference between a landscape cell and the nearest surface water cell along the local drainage path determined by the flow direction grid (Rennó et al., 2008).

2.5 Index aggregation

To better represent the SM pattern and answer the second research question, the index values were aggregated in hexagonal grids with a diameter of 100 meters. The individual index grid values were averaged using zonal statistics (ArcGIS Pro, Version 3.3.0). As the Kruskal-Wallis test (see Chapter 2.6) did not show significant differences between the two years, the temporal component could be neglected here and the values were averaged over both years to depict a more accurate long-term picture of the SM patterns in the area. For the aggregation, the normalized and inverted (see Chapter 2.6) values were classified into five quintiles.

2.6 Statistical evaluation

Different statistical components and figures were used to address the research questions. The programming environment RStudio (Version 2023.12.1+402) was employed here. As a basis for the analysis, random points were generated (n = 1000) to reduce computing time. Index values for all years and indices were extracted at the random point locations.

A preliminary data check with the Shapiro-Wilk (Shapiro & Wilk, 1965) and Levene test (Glass, 1966) showed heteroscedasticity and non-normal distribution of the residuals. Hence, the non-parametric Kruskal-Wallis test was applied (Kruskal & Wallis, 1952), followed by the Dunn test as post hoc (Dunn, 1964). To facilitate better interpretation and comparison, the index values were normalized using a linear min-max normalization. When interpreting SWI, higher values indicate wetter conditions, whereas for DTW and HAND, higher values represent drier conditions. Thus, DTW and HAND values were inverted after normalization to provide more meaningful and comparable results. All data and code can be found on the project's GitLab page (https://git.sbg.ac.at/st24_856165/topmod).

3 Results

Figure 2 shows the index maps for each index for both years. Visually examining the maps, one can see that the larger streams, lakes, and the Salzach are well identified by all indices.

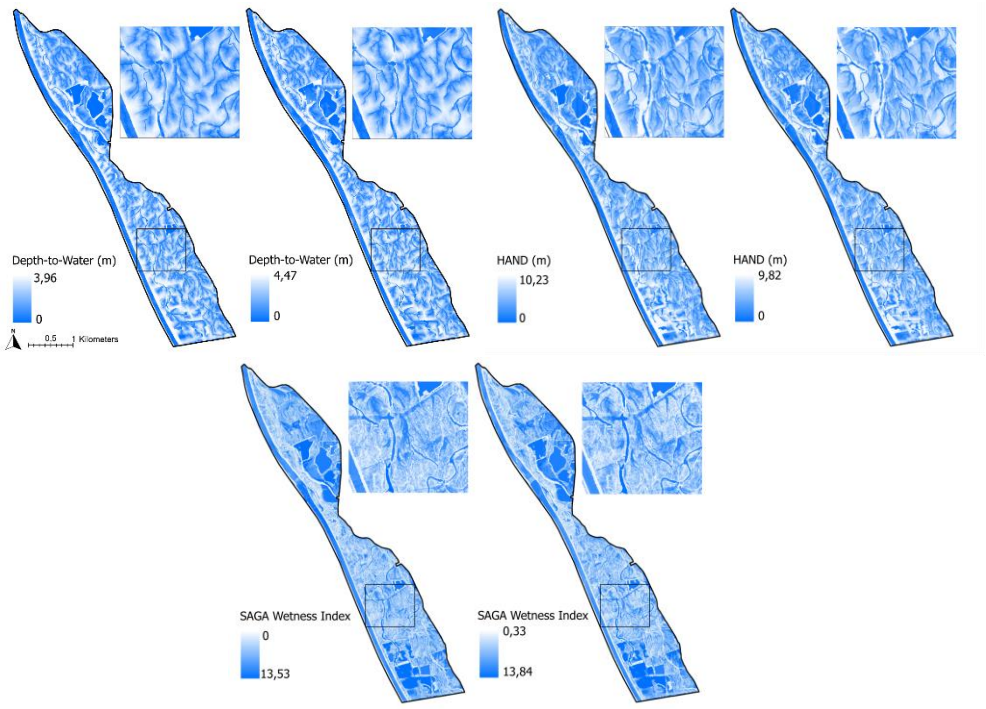

Figure 2: Index maps of the indices of 2016 (left) and 2022 (right), respectively.

However, the small streams in the SWI maps differ notably from those in the other two indices. Looking at the temporal component, there are barely any differences between the two years. However, there are noticeable differences in the fine patterns of the SM maps. The DTW primarily models wet areas near the stream channels, while the SWI shows contrasts between the stream channels and adjacent areas. This contrast is not observed along the Salzach river bank, where all indices model a strong contrast in SM.

Examining the statistics in Table 1, the SWI reaches mean values of 0.493 in 2016 and 0.497 in 2022, while the mean values for DTW and HAND are consistently higher at 0.829 and 0.888 (2016) and 0.829 and 0.887 (2022). The median values confirm this picture: the median of the SWI is 0.438 in 2016 and increases slightly to 0.452 in 2022, which is still well below the median values of DTW (0.871 in both years) and HAND (0.935 in 2016 and 0.933 in 2022). The standard deviations (SD) for SWI, DTW and HAND show different scatter patterns. The SWI has an SD of 0.231 in 2016 and 0.223 in 2022, which indicates moderate dispersion. In contrast, the DTW shows a lower standard deviation (0.175 in 2016 and 0.172 in 2022), and HAND shows the lowest (0.144 in 2016 and 0.145 in 2022). This pattern is also reflected in the boxplots (Fig. 3). The Kruskal-Wallis test revealed significant differences between the indices (p-value < 0.05). Post-hoc analysis using Dunn's test showed significant pairwise differences between all indices.

Table 1: Descriptive statistics of the index values. Mean and median of DTW und HAND were inverted to align with Fig. 3.

	SWI		DTW		HAND	
	2016	**2022**	**2016**	**2022**	**2016**	**2022**
Mean	0.493	0.497	0.829	0.829	0.888	0.887
Median	0.438	0.452	0.871	0.871	0.935	0.933
Standard deviation	0.231	0.223	0.175	0.172	0.144	0.145

In contrast, the Kruskal-Wallis test shows no statistically significant differences between the years (p-value = 0.6875). The mean values show that the SWI increased slightly in 2022 (0.497) compared to 2016 (0.493). The mean values for DTW and HAND in 2022 remain almost identical to the 2016 values, with DTW showing a value of 0.829 in both years and HAND showing a slight decrease from 0.888 to 0.887. The median values show an increase for the SWI from 0.438 in 2016 to 0.452 in 2022. The median for the DTW remains unchanged at 0.871, while the HAND median shows a minimal decrease from 0.935

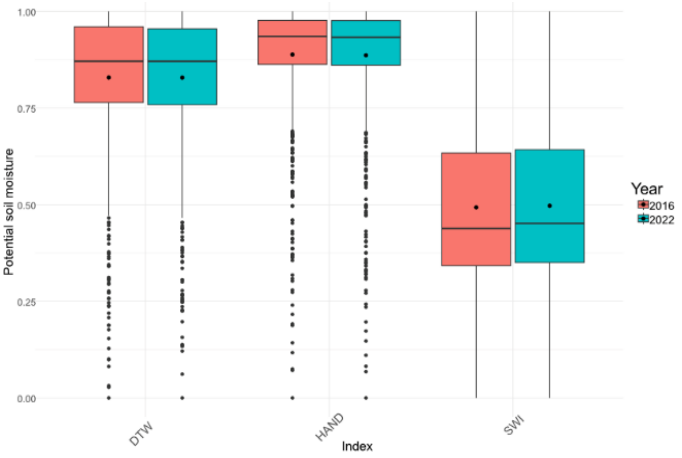

Figure 3: Boxplots of normalized and inverted index values.

in 2016 to 0.933 in 2022. The standard deviation (SD) for the SWI has decreased slightly, from 0.231 in 2016 to 0.223 in 2022, indicating a lower dispersion of the data in 2022. SD has decreased from 0.175 in 2016 to 0.172 in 2022 for the DTW. SD remains almost unchanged for HAND, with a minimal increase from 0.144 (2016) to 0.145 (2022).

The scatterplot matrix (Fig. 4) illustrates the pairwise relationships between the metrics DTW, HAND, and SWI for the years 2016 and 2022, along with their corresponding histograms and correlation coefficients. DTW and HAND display right-skewed distributions, indicating a higher frequency of lower values. In contrast, the SWI metric shows a more symmetric distribution for both years, with a slight skewness towards the centre. Cross-metric correlations reveal differing patterns. DTW and HAND metrics show strong positive correlations in both years, with ~0.8. Conversely, the correlations between DTW and SWI (~ -0.49), as well as HAND and SWI (~ -0.43), are moderately negative.

Examining the correlation coefficients between the years, we observe high positive correlations within the same metric over time. DTW shows a correlation of 0.94. Similarly, HAND (0.92) and SWI (0.91).

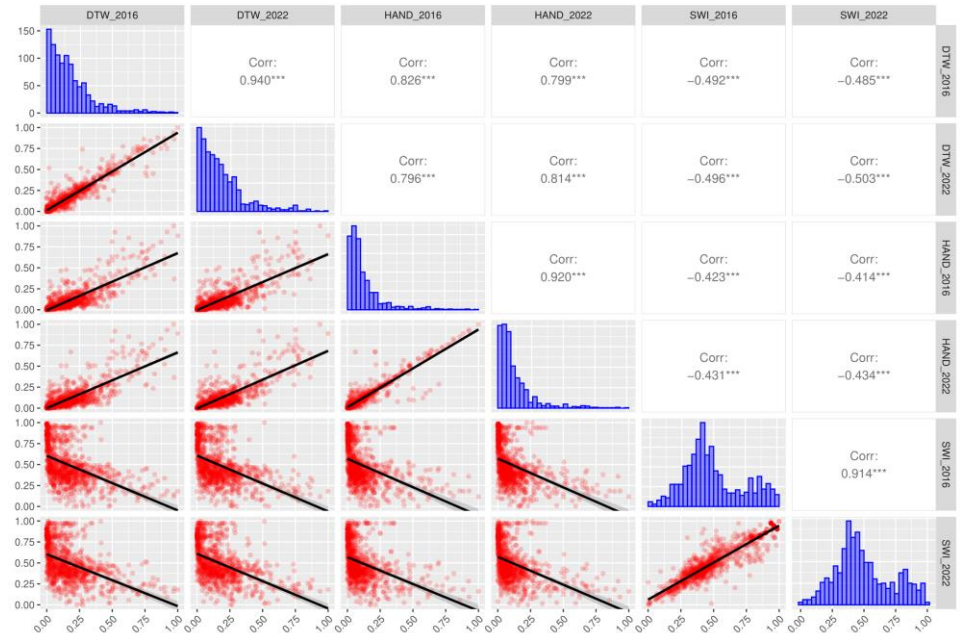

Figure 4: Scatterplot matrix of the indices.

Figure 5 depicts the distribution of SM across the study area. The maps show a heterogeneous SM pattern. However, all indices reveal a similar overarching pattern, with particularly moist locations in the northeastern part of the area and a dry ridge extending from south to north, right of the Salzach. While the patterns in the DTW and HAND maps are quite similar, the SWI estimates a very moist region in the southwestern part of the area. In contrast, HAND indicates a rather dry location in this region. The composite map presents a similar picture to

the other indices, highlighting particularly moist locations in the northeast and south of the area. The dry ridge is also clearly visible on this map.

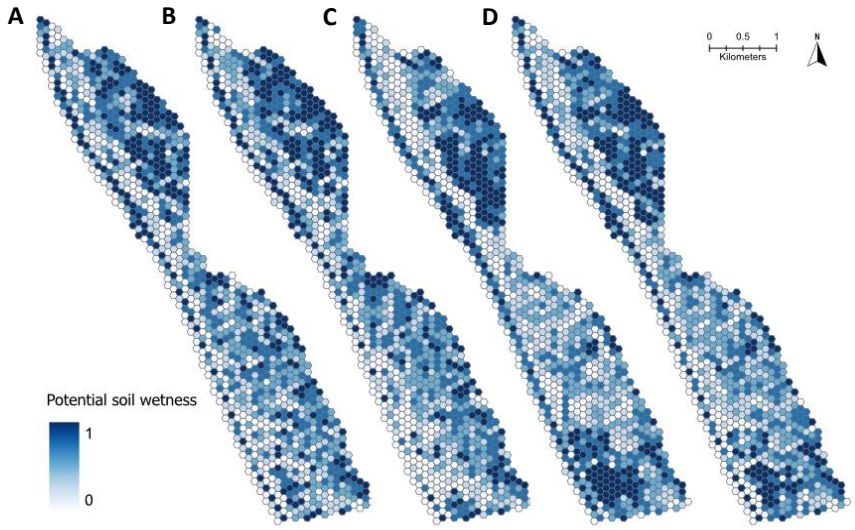

Figure 5: Soil moisture pattern in the study area of A) DTW B) HAND C) SWI D) All indices. A, B and C were averaged over years, D was averaged over indices and years.

4 Discussion

The results demonstrate the general suitability of the indices for small-scale, high-resolution SM modelling. Both the index value maps and the aggregated index maps show similar SM patterns, and larger streams, lakes, and the Salzach were well identified by all indices. The relatively dry areas to the right of the Salzach, identified by all indices, may be attributed to bank reinforcements in the area, which has been impacted by anthropogenic influences in the past (Strasser & Lang, 2015). Changes in maximum values between the years for the same index can be attributed to local renaturation measures or minor differences in data acquisition or processing. However, year-to-year differences are minimal, with only slight variations observed in central tendency and variability, suggesting data stability and robust index calculation.

The entire study hinges on the assumption that SM is strongly influenced by topography. Although other factors such as soil texture and type were not precisely incorporated into the methodology, it is reasonable to assume that topography significantly affects SM in the humid wetland study area. Furthermore, the small size of the study area indicates a uniformity of site conditions in terms of geological and soil properties. However, the incorporation of soil, climatic and other parameters for index calibration could enhance the study's accuracy and the index assessment since these parameters can strongly influence the impact of morphology on SM (Murphy et al., 2009).

Although the selected method gives a good overview of wet and dry soil conditions, the results are less indicative for deeper soil layers, as the influence of topography decreases with depth (Oltean et al., 2016). Moore et al. (1993) found that TWI and other terrain attributes explained significant variations in soil properties, with the strongest correlations in the organic horizon.

The distributions of values for DTW and HAND are notably right-skewed, with many values near zero. This can be explained by the flat terrain and the high groundwater levels described by the BFW (2023). Despite the significant differences in the central tendencies of the indices' values, the moderate to strong correlations between the indices underscore their suitability for the test area and the spatial resolution of the data. The correlation of SWI with the other indices is surprising, since, for instance, Nobre et al. (2011), did not find a correlation between HAND and TWI. Additionally, previous studies indicate the unreliability of the TWI when calculated on high-resolution DEMs (Ågren et al., 2021). The moderate correlation in this study could be possibly due to the modified calculation of the SWI's specific catchment area, which improves the flow modelling of water in flat areas (Böhner & Selige, 2002). This could have improved the SWI's performance in the floodplain area, although TWI generally performs poorly in flat areas (Mattivi et al., 2019).

Next to these factors, the results of the SWI calculation are significantly influenced by the chosen parameters and the specific environmental context, hampering index calibration and influencing the results. Establishing a universal calculation method for TWI parameters is challenging due to its inherent scale dependency and the variability in methods used for computing drainage paths. Additionally, the optimal resolutions for TWI calculations can vary depending on the landscape (Ågren et al., 2015), and TWI itself fluctuates with changes in landscape, climate, and scale (Mattivi et al., 2019).

Thus, the results of HAND and DTW in this study are probably more valid than those of the SWI. HAND offers more universal climatic and scale-independent applicability due to the constant reference point provided by the drainage network (Nobre et al., 2011). The DTW index has proven applicable to flat areas (Echiverri & Macdonald, 2019), particularly in riparian forests and formerly glaciated landscapes in Scandinavia (Larson et al., 2022). Moreover, DTW is particularly accurate when using high-resolution LiDAR DEMs (Murphy et al., 2009). However, the results of the DTW and HAND maps are heavily dependent on the chosen FIA for stream extraction. Lower FIA values result in more predicted streams and wetter modelled outcomes for DTW and HAND. In this study, the FIA was selected after a literature review and by considering the humid site conditions. Nevertheless, there is still a seasonal bias (Ågren & Lidberg, 2019), and FIA selection is often prone to errors, resulting in over- or underestimation of streams. Since a small FIA was chosen for this study, there is a potential overestimation of streams. This could also have led to DTW and HAND estimating the area as wetter overall, while the SWI modeled drier values. Reference data such as groundwater level measurements or field data are therefore required to further validate the indices. Furthermore, it highlights the need for further research on the FIA on the index results in the study area.

5 Conclusion and Outlook

This study compared topography-based approaches for SM estimation using high-resolution DEMs in a small-scale floodplain area. Visual and statistical index validation demonstrates general suitability of the indices for SM modelling, evidenced by similar SM patterns and moderate to strong correlations across the indices. However, as the SAGA Wetness Index differs most from the other two indices and it is sensitive to climate and scale, it should be applied with careful consideration. Here, further index validation and the incorporation of reference data are necessary to enhance the accuracy of the assessment.

Further research must examine the influence of the FIA on the results and integrating climatic, hydrographic, and soil parameters would improve index accuracy and applicability. Additionally, incorporating seasonal changes in SM regimes into the index calculation workflow could also provide more accurate patterns and adapt decision-making to temporal differences.

Acknowledgements

I would like to thank Assoc. Prof. Dr. Hermann Klug and Dr. Thomas Strasser for their advice and feedback throughout the project, which contributed to the development of the results.

References

Ågren, A., & Lidberg, W. (2019). The importance of better mapping of stream networks using high resolution digital elevation models – upscaling from watershed scale to regional and national scales. *Hydrology and Earth System Sciences Discussions*, 1-20. https://doi.org/10.5194/hess-2019-34

Ågren, A., Lidberg, W., & Ring, E. (2015). Mapping Temporal Dynamics in a Forest Stream Network—Implications for Riparian Forest Management. *Forests*, *6*, 2982-3001. https://doi.org/10.3390/f6092982

Ågren, A. M., Larson, J., Paul, S. S., Laudon, H., & Lidberg, W. (2021). Use of multiple LIDAR-derived digital terrain indices and machine learning for high-resolution national-scale soil moisture mapping of the Swedish forest landscape. *Geoderma*, *404*, 115280. https://doi.org/https://doi.org/10.1016/j.geoderma.2021.115280

Bell, J. C., Cunningham, R. L., & Havens, M. W. (1992). Calibration and validation of a soil-landscape model for predicting soil drainage class. *Soil Science Society of America Journal*, *56*(6), 1860-1866.

Beven, K. J., & Kirkby, M. J. (1979). A physically based, variable contributing area model of basin hydrology / Un modèle à base physique de zone d'appel variable de l'hydrologie du bassin versant. *Hydrological Sciences Bulletin*, *24*(1), 43-69. https://doi.org/10.1080/02626667909491834

BFW. (2023). *"eBOD". Digitale Bodenkarte Österreichs.* https://bodenkarte.at

Bhowmik, A. K., Metz, M., & Schäfer, R. B. (2015). An automated, objective and open source tool for stream threshold selection and upstream riparian corridor

delineation. *Environmental Modelling & Software*, *63*, 240-250. https://doi.org/https://doi.org/10.1016/j.envsoft.2014.10.017

Böhner, J., & Selige, T. (2002). Spatial prediction of soil attributes using terrain analysis and climate regionalization. *Gottinger Geograpihsche Abhandlungen*, *115*.

Dilts, T. (2023). *Topography Toolbox for ArcGIS Pro*. In University of Nevada Reno https://www.arcgis.com/home/item.html?id=247fbe56c7ff48229c9b1fe132d1b5e9

Dunn, O. J. (1964). Multiple Comparisons Using Rank Sums. *Technometrics*, *6*(3), 241-252. https://doi.org/10.1080/00401706.1964.10490181

Echiverri, L., & Macdonald, S. E. (2019). Utilizing a topographic moisture index to characterize understory vegetation patterns in the boreal forest. *Forest Ecology and Management*, *447*, 35-52. https://doi.org/https://doi.org/10.1016/j.foreco.2019.05.054

Famiglietti, J. S., Rudnicki, J. W., & Rodell, M. (1998). Variability in surface moisture content along a hillslope transect: Rattlesnake Hill, Texas. *Journal of Hydrology*, *210*(1), 259-281. https://doi.org/https://doi.org/10.1016/S0022-1694(98)00187-5

Glass, G. V. (1966). Testing Homogeneity of Variances. *American Educational Research Journal*, *3*(3), 187-190. https://doi.org/10.3102/00028312003003187

Hengl, M., Aufleger, V. d. M., Eggersberger, J., Hafner, T., Michor, K., Mühlbacher, M., Raudaschl, S., Schuardt, W., Spannring, M., Unterlercher, M., & Wiesenegger, C. (2012). Eigendynamische Aufweitungen an der Unteren Salzach - vom Konzept bis zu den ersten Erfahrungen. *Oesterr. Wasser- Abfallwirtsch.* , *64*(7-8), 401-410.

Johnson, J. M., Munasinghe, D., Eyelade, D., & Cohen, S. (2019). An integrated evaluation of the National Water Model (NWM)–Height Above Nearest Drainage (HAND) flood mapping methodology. *Nat. Hazards Earth Syst. Sci.*, *19*(11), 2405-2420. https://doi.org/10.5194/nhess-19-2405-2019

Kruskal, W. H., & Wallis, W. A. (1952). Use of Ranks in One-Criterion Variance Analysis. *Journal of the American Statistical Association*, *47*(260), 583-621. https://doi.org/10.1080/01621459.1952.10483441

Larson, J., Lidberg, W., Ågren, A. M., & Laudon, H. (2022). Predicting soil moisture conditions across a heterogeneous boreal catchment using terrain indices. *Hydrol. Earth Syst. Sci.*, *26*(19), 4837-4851. https://doi.org/10.5194/hess-26-4837-2022

Lidberg, W., Nilsson, M., & Ågren, A. (2020). Using machine learning to generate high-resolution wet area maps for planning forest management: A study in a boreal forest landscape. *Ambio*, *49*(2), 475-486. https://doi.org/10.1007/s13280-019-01196-9

Lidberg, W., Nilsson, M., Lundmark, T., & Ågren, A. M. (2017). Evaluating preprocessing methods of digital elevation models for hydrological modelling. *Hydrological Processes*, *31*(26), 4660-4668. https://doi.org/https://doi.org/10.1002/hyp.11385

Lindsay, J. B. (2016). Efficient hybrid breaching-filling sink removal methods for flow path enforcement in digital elevation models. *Hydrological Processes*, *30*(6), 846-857. https://doi.org/https://doi.org/10.1002/hyp.10648

Mattivi, P., Franci, F., Lambertini, A., & Bitelli, G. (2019). TWI computation: a comparison of different open source GISs. *Open Geospatial Data, Software and Standards*, *4*(1), 6. https://doi.org/10.1186/s40965-019-0066-y

Mohtashami, S., Eliasson, L., Hansson, L., Willén, E., Thierfelder, T., & Nordfjell, T. (2022). Evaluating the effect of DEM resolution on performance of cartographic depth-to-water maps, for planning logging operations. *International Journal of Applied Earth Observation and Geoinformation*, *108*, 102728. https://doi.org/https://doi.org/10.1016/j.jag.2022.102728

Moore, I. D., Gessler, P., Nielsen, G. A. E., & Peterson, G. (1993). Soil Attribute Prediction Using Terrain Analysis. *Soil Science Society of America Journal - SSSAJ, 57*. https://doi.org/10.2136/sssaj1993.572NPb

Murphy, P. N. C., Ogilvie, J., & Arp, P. (2009). Topographic modelling of soil moisture conditions: a comparison and verification of two models. *European Journal of Soil Science*, *60*(1), 94-109. https://doi.org/https://doi.org/10.1111/j.1365-2389.2008.01094.x

Murphy, P. N. C., Ogilvie, J., Connor, K., & Arp, P. A. (2007). Mapping wetlands: A comparison of two different approaches for New Brunswick, Canada. *Wetlands*, *27*(4), 846-854. https://doi.org/10.1672/0277-5212(2007)27[846:MWACOT]2.0.CO;2

Nobre, A., Cuartas, L., Hodnett, M., Rennó, C., Medeiros, G., Silveira, A., Waterloo, M. J., & Saleska, S. (2011). Height Above the Nearest Drainage - a hydrologically relevant new terrain model. *Journal of Hydrology*, *404*, 13-29. https://doi.org/10.1016/j.jhydrol.2011.03.051

O'Callaghan, J. F., & Mark, D. M. (1984). The extraction of drainage networks from digital elevation data. *Computer Vision, Graphics, and Image Processing*, *28*(3), 323-344. https://doi.org/https://doi.org/10.1016/S0734-189X(84)80011-0

Oltean, G. S., Comeau, P. G., & White, B. (2016). Linking the Depth-to-Water Topographic Index to Soil Moisture on Boreal Forest Sites in Alberta. *Forest Science*, *62*(2), 154-165. https://doi.org/10.5849/forsci.15-054

Rennó, C. D., Nobre, A. D., Cuartas, L. A., Soares, J. V., Hodnett, M. G., Tomasella, J., & Waterloo, M. J. (2008). HAND, a new terrain descriptor using SRTM-DEM: Mapping terra-firme rainforest environments in Amazonia. *Remote Sensing of Environment*, *112*(9), 3469-3481. https://doi.org/https://doi.org/10.1016/j.rse.2008.03.018

Schönauer, M., Ågren, A. M., Katzensteiner, K., Hartsch, F., Arp, P., Drollinger, S., & Jaeger, D. (2024). Soil moisture modeling with ERA5-Land retrievals, topographic indices, and in situ measurements and its use for predicting ruts. *Hydrol. Earth Syst. Sci.*, *28*(12), 2617-2633. https://doi.org/10.5194/hess-28-2617-2024

Schönauer, M., Väätäinen, K., Prinz, R., Lindeman, H., Pszenny, D., Jansen, M., Maack, J., Talbot, B., Astrup, R., & Jaeger, D. (2021). Spatio-temporal prediction of soil moisture and soil strength by depth-to-water maps. *International Journal of Applied Earth Observation and Geoinformation*, *105*, 102614. https://doi.org/https://doi.org/10.1016/j.jag.2021.102614

Shapiro, S. S., & Wilk, M. B. (1965). An analysis of variance test for normality (complete samples)†. *Biometrika*, *52*(3-4), 591-611. https://doi.org/10.1093/biomet/52.3-4.591

Strasser, T., & Lang, S. (2015). Object-based class modelling for multi-scale riparian forest habitat mapping. *International Journal of Applied Earth Observation and Geoinformation*, *37*, 29-37. https://doi.org/https://doi.org/10.1016/j.jag.2014.10.002

Yin, S., Bai, J., Wang, W., Zhang, G., Jia, J., Cui, B., & Liu, X. (2019). Effects of soil moisture on carbon mineralization in floodplain wetlands with different flooding frequencies. *Journal of Hydrology*, *574*, 1074-1084. https://doi.org/https://doi.org/10.1016/j.jhydrol.2019.05.007